Journal of Engineering for Gas Turbines and Power. Received July 18, 2023;
Accepted manuscript posted October 18, 2023. doi:10.1115/1.4063785

THE APPLICATION OF AN ARTIFICIAL NEURAL NETWORK AS A BASELINE MODEL FOR CONDITION MONITORING OF INNOVATIVE HUMIDIFIED MICRO GAS TURBINE CYCLES

Kathryn Colquhoun

Faculty of Science and Technology, University of Stavanger

Stavanger, Norway

Homam Nikpey Somehsaraei

Faculty of Science and Technology, University of Stavanger

Stavanger, Norway

Ward De Paepe[1]

Thermal Engineering and Combustion Research Unit, University of Mons

Mons, Belgium

ABSTRACT

Due to high penetration of renewables, the EU energy system is undergoing a transition from large-scale centralized generation towards small-scale distributed generation. The increasing share of intermittent renewables such as solar and wind has become the main driver for dispatchable distributed energy generation technologies to maintain the grid flexibility and stability. In this context, micro gas turbines (MGTs) with high fuel and operation flexibility could play a crucial role to guarantee the grid stability, enabling deeper penetration of the intermittent renewable energy sources.

Despite this, the MGT market is still considered to be niche and there are R&D&I challenges that need to be addressed to further promote this technology in distributed generation applications. Innovative MGT cycles based on a cycle humidification concept, can be considered to obtain higher system performance. However, given the fact that

[1] Address all correspondence to this author. Tel: +32 (0)65/37.44.71 Email: ward.depaepe@umons.ac.be

MGTs are installed close to the consumption points, where they are operated by non-technical prosumers with very limited access to maintenance services, they should also offer high availability and reliability to avoid unexpected outages and secure the supply. Therefore, intelligent monitoring systems are needed that can support non-expert end-users to detect degradation and plan maintenance before a breakdown occurs.

In this study we investigated and developed advanced methods based on artificial neural networks (ANNs) for condition monitoring of a humidified MGT cycle under real-life operational conditions. To create a high-performing model, extensive data preprocessing has been conducted to remove data outliers and select optimum model features, which provide best results. Additionally, the model hyperparameters such as learning rate, momentum and number of hidden nodes have been altered to achieve the most accurate predictions. The results of this study have provided a baseline ANN model capable of conducting condition monitoring of a micro-Humid Air Turbine (mHAT) system, which will be applied to additional studies in the future.

Keywords: micro gas turbine, ANN, innovative cycles, mHAT cycle

NOMENCLATURE

ANN	Artificial Neural Network
CCHP	Combined Cooling Heat and Power
CCIT	Combustion Chamber Inlet Temperature
CHP	Combined Heat and Power
CIP	Compressor Inlet Pressure
COP	Compressor Outlet Pressure
COT	Compressor Outlet Temperature
C_p	Specific Heat Constant for Constant Pressure
EIT	Economizer Inlet Temperature
GD	Gradient Descent
GT	Gas Turbine
KF	Kalman Filter
MAE	Mean Absolute Error
MFANN	Multi Feed Forward Artificial Neural Network
MGT	Micro Gas Turbine

mHAT	micro–Humid Air Turbine
ML	Machine Learning
MLP	Multi-Layer Perceptron
MSE	Mean Squared Error
N	Engine Rotational Speed
NN	Neural Network
P_{amb}	Ambient Pressure
P_{gen}	Generated Power
P_{req}	Requested Power
RIT_a	Recuperator Air Inlet Temperature
RE	Relative Error
RMSE	Root Mean Square Error
TIT	Turbine Inlet Temperature
TOT	Turbine Outlet Temperature
T_{wIn}	Water temperature entering system
T_{wSatIn}	Water temperature entering saturation tower
T_1 (CIT)	Compressor Inlet Temperature
V_{wSat}	Injection flow rate of water in saturation tower
W	Weights
ΔP	Pressure difference over fine filter
f	Activation Function

INTRODUCTION

With a global population devoted to reducing environmental impact on the earth, it is no wonder that renewables have become so popular in recent years. In face of the unexpected and economically challenging times through 2020 and 2021, due to COVID-19, still a substantial amount of renewable power sources was commissioned. Totally, 200GW and 290GW of new renewable power was installed in 2020 and 2021, respectively, and of this, solar amounted to more than half, closely followed by wind [1]. However, these resources are intermittent and in order to meet

electrical demand and stabilize the grid, other dispatchable distributed generation units, such as hydropower and micro gas turbines (MGT), must be optimized.

MGTs have become more popular due to their operation and fuel flexibility, low emissions, low maintenance and short ramp up times. They are particularly popular for their use in producing Combined Heat and Power (CHP) and Combined Cooling Heat and Power (CCHP), producing between 3kW and 250kW of electrical power and up to 450kW in heat. They can also be combined to operate in parallel where the total electrical output could reach up to 1,000kW [2].

Traditional MGTs operate on natural gas, but the combustion process produces toxins which are harmful to the environment, such as CO_2 and NO_x. Advances have now taken place that allow MGTs to become more environmentally friendly permitting the use of different combinations of fuel, for example biogas and hydrogen, while still operating at full capacity [3–6]. However, despite some distinct advantages of MGTs over other kinds of heat engines in terms of atmospheric emissions, fuel flexibility, noise, size, and vibration levels [7], their electrical efficiency is still lower, while investment costs are similar [8]. Efficiency can be improved in many ways by upgrading system components – specifically, using materials which can withstand higher temperatures, installing a fuel flexible combustion chamber, and increasing the effectiveness of the recuperator.

More recently work has been conducted to explore the benefits of running MGTs on more innovative cycles than that of the traditional Brayton Cycle [9–13]. One option is to humidify the air with the addition of an economizer and saturation tower into the system. This produces the micro-Humid Air Turbine (mHAT) cycle, which has shown promising results, including higher electrical efficiency, cleaner exhaust, and lower emissions. Additionally, humidification allows for more flexibility towards heat and power production, resulting in lower heat demand dependence than the traditional MGTs.

However, humidifying the cycle changes the operating conditions of the MGT, which can cause problems in performance. Adding water to the cycle causes the mass flow rate of the working fluid to change. Considering that the turbine limits the total mass flow rate of working fluid, any water addition behind the compressor, as is the case in cycle humidification, will lead to a reduction in compressor mass flow rate and thus pushes the compressor operating point closer to the surge margin [14]. Given the missing information on this reduction, surge events are hard to predict. Additionally, the higher specific water content changes the working fluid C_p and thus affects the combustion efficiency and flame stability [15]. Due to the increased C_p, the temperature levels in the combustion chamber are lower, leading

to reduced reaction rates and thus lower efficiency and higher CO emissions [16]. In the case of too high water fraction, an extinction of the flame or so-called flame-out can occur [17][18]. Considering the altered engine dynamics due to the introduction of a large volume between compressor outlet and recuperator inlet [19], requiring a specific startup and shutdown procedure with blow-off valve opening to prevent surge [20], any event leading to an unexpected and unpredictable engine shut down, such as this flameout, must be avoided. Unfortunately, no option for flame-out detection is currently available that allows for sufficiently fast control action to avoid this surge[2]. Consequently, to avoid surge of any kind of the compressor, it is important to constantly monitor the system to ensure no large deviations in measurable parameters and guarantee that technology is available, which is capable of notifying end-users of arising faults. This results in better maintenance planning and, in turn, reduces costs due to loss in production.

Over the years both model-based and data-driven approaches have been employed to optimize condition-based monitoring and fault diagnostics, with data-driven methods becoming more popular in recent studies. A study comparing model-based and data-driven approaches for gas turbine gas path components was explored by Volponi et al. [1]. It studied a comparison between three different methods on an aero propulsive GT: the Kalman filter (KF), an MLP with back propagation, and a hybrid ANN. These models were used to detect single faults at the component level. The hybrid ANN encompassed both data-driven and model-based methods, by including influence coefficient matrices that were used in the KF. Of the three, the hybrid ANN produced the highest accuracy results when considering the gas turbine to be a linear problem.

More recently, a degradation detection study of a gas turbine compressor and turbine was performed by Hanachi et al. [21]. An adaptive neuro-fuzzy inference system was used, and data was obtained for varying severity of component degradation. It was discovered that the system was able to detect and estimate the level of degradation in a component well, but overall accuracy improved when the degraded component was identified in advance. Additionally, including the turbine mass flow rate and TIT as parameters further increased the model diagnostic performance.

When focusing on work using ANNs, it is clear that MLP networks, also referred to as Multi feedforward artificial neuron networks (MFANN) in some cases, are one of the most common architectures to use, with multiple studies utilizing this method [22–24]. Yoon et al. focused on compressor, turbine, and recuperator degradation detection within an MGT using an MLP network [25]. A physical simulation, based on a real 30kW MGT, was run for different

[2] For a full in-depth discussion of the impact of humidification on the MGT and its components, we refer to [8]

degradation scenarios and the data generated was used in the ANN. The number of input and hidden neurons were altered to find the optimum model and it was discovered that the model with the highest number of inputs (nine) was the most accurate model. However, the models with between five and eight inputs also had good results; with a Root Mean Squared Error (RMSE) less than 1%. Hamouda et al. created a three ANN classifier system that was able to detect different modes of operation of an MGT. It then used this to adapt the control system using a minimum number of features [26]. This system was able to perform accurate classification when operating in online mode.

An MLP study was performed by Nikpey et al. [22], where the network was used to monitor an MGT operating at its steady state conditions. The MLP was trained and validated via back propagation and utilized data from a modified Turbec T100 MGT. Through this study it was found that the optimum inputs were CIT, CIP, P_{req} and fuel temperature; while the outputs were P_{gen}, COP, COT, TOT, CCIT, CCIP, hot water temperature and oil temperature. Results illustrated that this MLP network was able to accurately predict normal performance of the MGT and could be used for online monitoring in the future. This study was useful in providing a set of desired inputs and outputs for an effective ANN, which monitors the performance of a MGT when fueled on pure natural gas.

Considering the studies mentioned previously, it is clear that ANNs perform well for condition monitoring and fault diagnostics for traditional MGT systems. Therefore, it makes sense to assess their ability to perform this task on an innovative mHAT cycle.

This work focuses on how ANNs can be used to monitor a MGT operating on a HAT cycle and optimal model features will be recommended, which provide the best performance. This was enabled due to the availability of the extensive measured data obtained from a humidified MGT test rig at the Vrije Universiteit Brussel (VUB) in Belgium. The knowledge and competence developed in this study will pave the way for building up an accurate and reliable baseline model for system monitoring in real-time applications. This study is the first step in a series of research utilizing data-driven methods for modeling and monitoring of distributed generation units based on humidified MGT systems. This paper will be used as a reference for additional studies to be conducted in future.

The outline of the paper is as follows: Description of MGT and mHAT system; overview of ANNs and how the data has been split; preprocessing and preparation of the data; training process and optimization of the ANN; results and discussion of the final model; and ideas for future studies.

SYSTEM DESCRIPTION

The system considered in this work is the T100 humidified MGT test rig of the VUB [6, 10] . The basis of the test rig is a classical Turbec T100 series 2 MGT (nominal power of 100kW$_e$) operating according to the recuperated Brayton cycle (black parts in Figure 1). Air is first compressed in a variable speed radial compressor, then preheated by the flue gases in a mixed cross and counter-flow heat exchanger (recuperator), before entering the combustion chamber where natural gas is burned to increase the Turbine Inlet Temperature (TIT) to 950°C. The hot gases are expanded over the turbine, to deliver mechanical power to drive both the compressor and the high-speed generator (for electrical power production). After passing through the recuperator, the remaining heat in the flue gases is transferred into thermal power by heating water in the economizer. In the HAT layout, this thermal power is reintroduced in the cycle by means of a saturation tower, located in between the compressor outlet and the recuperator inlet, allowing to humidify the compressed working fluid, and by doing so, improving the electrical performances of the cycle [8]. For the VUB test rig, a specific crossflow spray saturation tower (without packing material to limit the pressure drop) was developed [27] and integrated. The performance of the cycle [12] as well as the recuperator [28] and saturation tower [29] under humidified conditions has been tested and validated extensively.

The test rig is equipped with a Data Acquisition system and sensors to measure the impact of cycle humidification on both cycle performance, as well as individual component performance. This includes temperature sensors at each component inlet and outlet for both the gas path (except for the turbine inlet) as well as the water circuit; pressure sensors at the compressor inlet and outlet; and flow sensors to measure the injected water mass flow rate as well as the consumed natural gas flow rate. Finally, rotational speed sensors and electrical power measurements allow for identification of the impact of the humidification on the global cycle performance (a complete list of installed sensors, including the type and their accuracy is presented in [12]). Furthermore, the cycle is equipped with a series of valves, that can be activated to bypass the saturation tower (to operate in normal dry mode), as well as bleed and blowoff valves, installed to protect the compressor against surge during humidified operation and shutdown respectively.

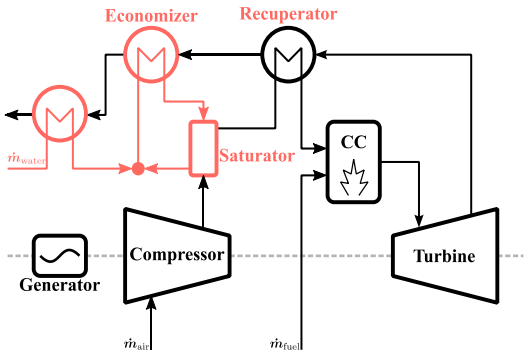

Figure 1 The Turbec T100 operating using the recuperated Brayton cycle is converted into a HAT cycle by introducing a spray saturation tower between compressor outlet and recuperator inlet, allowing for humidification of the compressed air

The Turbec T100 has a specific control system, composed of two main loops: TOT control and power output control. The TOT is kept constant at 645°C by altering the valve opening time of the fuel valves of the combustion chamber, changing the injected natural gas flow rate and while doing so, altering the thermal input of the combustion chamber. Second, the power output of the engine is kept constant by changing the rotational speed of the shaft. This combined TOT and power control allows for efficient nominal and part-load operation. For the VUB test rig, the TOT control was kept, while the power control was slightly altered, also allowing for operation at constant rotational speed.

Tests are typically performed by starting the engine using a dedicated start-up procedure (described in [30]) including water injection prior to the engine start in the saturation tower. After reaching steady state, the engine is typically run for at least 30 minutes at a predefined power output (constant power mode) or rotational speed (constant speed mode) with constant and stable water injection, before a switch to a new setpoint is made. During these tests, all cycle parameters are captured with a sampling ratio of 10Hz. To protect the compressor against surge, during wet operation, the bleed valve is systematically partially opened, creating additional surge margin. As highlighted in the introduction, due to the water addition behind the compressor, the compressor operating point is shifted and by doing so, reduces the surge margin[8]. Finally, after finishing the tests, a controlled shutdown is performed. During this shutdown, the blowoff valve is opened, again to protect the compressor from going into surge. Due to the addition of an extra volume in between compressor outlet and recuperator inlet, the transient behaviour of the system has altered drastically. The pressurized air in the volume needs to be discharged to the turbine as well, so that during a shutdown, the backpressure of the compressor is too high and thus leads to surge. By opening a blowoff valve, this could be avoided[3] [30].

[3] For a more in-depth discussion on the impact of humidification and pressure loss on surge margin as well as on its control, we refer to [31].

Despite the dedicated operating and shutdown strategy using bleed and blow off valves to protect the compressor against surge, so far, no protection against unexpected shutdowns, due to combustor flame out, is currently installed on the system, leaving it still exposed. As a result of the humidification of the working fluid, the composition of the combustion air entering the combustor is altered. The additional water fraction negatively impacts the combustion efficiency and stability. Under normal operating conditions (100% humidified), the combustion chamber is capable of maintaining the flame while still presenting high combustion efficiency (>99%); however, during start-up phase, load changes or over-saturation (meaning liquid water entering the recuperator after the saturation tower[4]), experience has shown that there is an increased risk for flameout. To protect the compressor during such a flameout, it is crucial that the flameout is detected rapidly, allowing for the blow-off valve to be opened before the compressor goes into surge. However, this requires the installation of a flame sensor in the chamber, which is technically challenging. Previous efforts using alternative indirect flame-out measurement (TOT, pressure, or rotational speed drop) have proven ineffective, since surge occurs before a significant drop can be observed. Nevertheless, from prior analysis, it was found that flame out is typically linked with too low CIT or a specific imbalance in CIT after the recuperator [12]. Hence, although the direct measurement of this imbalance does not allow for the development of a specific emergency control, given the uncertainty on the measurements, it is expected that by using an ANN, potentially upcoming flameout can be predicted with better accuracy and fast enough, allowing to protect the compressor.

METHODOLOGY

This paper investigates the use of ANN for monitoring of a humidified micro gas turbine. The real-life data obtained from the test rig described in the preceding section was used for this purpose. The analysis of the data showed highly nonlinear variations of the operational parameters. The selection of the required inputs and desired outputs resulted in a multidimensional model structure. Given that ANNs have shown very good performance in prediction of the nonlinear and multidimensional systems, they have been selected for this study.

The ANN model can be used as a baseline model, providing the possibility to design a fast and user-friendly monitoring tool for real-time application. All the steps of data processing and model optimization are discussed in the following sections.

[4] For a full discussion on oversaturation, we refer to [29].

Artificial Neural Network

An ANN is a type of ML technique, where a computer is configured to perform in a way that is similar to how the human brain functions. It is made up of many artificial neurons, or nodes, which process information as it passes through the various layers in the architecture. One type of ANN is a feed-forward neural network, or MLP, illustrated in Figure 2, where each neuron in one layer passes information to the neurons in the proceeding layer via linear or nonlinear transfer functions. The network requires an input of data to train the algorithm in understanding how a particular system operates, then it can provide a set of predicted outputs. Each individual connection is assigned its own weight, and during the training process these weights are altered and optimized as the algorithm learns how to find the best output based on a given input. This type of ANN has proven to be one of the most popular techniques within condition monitoring and fault diagnostics in MGTs.

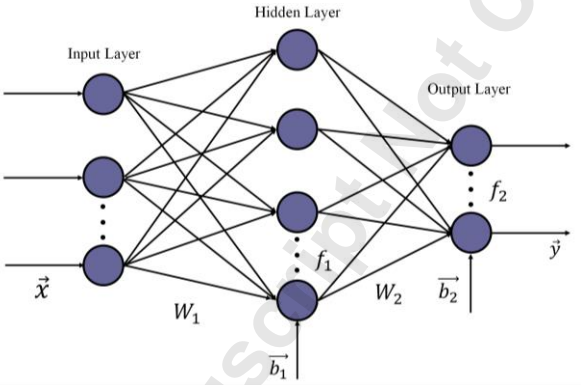

Figure 2 Multilayer Perceptron network structure

In this work, a 1-hidden layer ANN was created using the popular ANN library, Keras, within Python. The code was written on Jupyter Notebook, due to its user-friendly set up and ease to run and edit code. Additionally, Tensorboard was used to evaluate and compare the loss and accuracy of different models during the optimization process. The weights were optimized through a process known as back propagation. This is where the derivative of the loss between true and predicted outputs is found and propagated back through the model to update the weights at each layer.

Often when creating an ANN, it can seem as if the training error is very low, but when the network is tested on unseen data it does not generalize well due to overfitting of the training set. One way to avoid this is to split the overall data into a training, validation and testing set. There are a few different ways to split the data into the required sets. The most common is to split the data randomly, which is a suitable option when a significant amount of data is available. If there is not a large quantity of data, as was the case for this study, then there is the risk of having sampling

bias as the test set may not represent the overall dataset patterns. It was difficult to obtain a significant amount of data for this fault as it would put the MGT at serious risk. An alternative method is to use stratified sampling. This process involves selecting an important feature of the system and dividing it into equal strata. Then the data is split so that the same number of samples from each stratum are included in the training and testing sets. This guarantees that the test set is representative of the whole data set.

A small investigation was conducted to determine the error in distribution of data when using random and stratified sampling methods. The data was stratified according to multiple different parameters, and it was discovered that stratifying according to the compressor inlet temperature, T_1, was most appropriate. T_1 was split into 4 categories and Table 1 compares the category proportions of the overall dataset with the test set for both sampling techniques. The results from this show that stratified sampling has a more similar data distribution to the overall dataset than using random sampling. Therefore, this method was used to split the test set.

Table 1 Comparison of the T_1 category proportions in the overall data set and the test set using random and stratified sampling methods

	Overall	**Stratified**	**Random**	**Stratified % error**	**Random % error**
1	0.272759	0.272780	0.272416	0.007774	-0.125854
2	0.407170	0.407202	0.408879	0.007826	0.419602
3	0.153540	0.153521	0.150095	-0.012411	-2.243853
4	0.166531	0.166497	0.168611	-0.020425	1.249017

The validation set is a subset of the training set, used to evaluate the model at each step, while model parameters are updated during training. Generally, a model with low training and validation error should perform well on the test set and so can generalize well to unseen samples. In this work a total of 68,621 samples were used. The training set was made up of 60% of this data, while the remaining 40% was evenly split between the validation and test set.

The next section discusses the steps of pre-processing the data before it is fed into the model. It is important to be aware that the data exploration was only carried out on the training and validation set to avoid data snooping bias on the test set, which could result in an overfit network.

Data Processing, Preparation & Filtering

The used data was captured on the T100 HAT test rig under humidified conditions. The engine was operating at constant TOT and constant power output, while water was injected in the spray saturation tower to humidify the air. The water flow rate was controlled manually by altering the pump speed and the number of used injection nozzles,

ensuring continuous injection, while ensuring a fine fog for optimized heat and mass transfer. As mentioned before, a sample frequency of 10Hz was used to capture the data. During the tests used for the analysis presented in this paper, the water mass flow rate was increased progressively, until a maximal injection flow rate of 2.5 kg/s was reached or an unexpected flame-out occurred.

Before a model could be trained and optimized it was important to ensure the data being fed into the algorithm was properly prepared. Firstly, the choice of input and output features was considered. This involves understanding the operation of the system and how measurable parameters relate to each other. To ensure optimum features were selected, feature transformations were conducted and the correlation between input and output parameters found. The final input and output features can be found in Table 2. The reason for selecting two EIT features, was due to sensors being placed at the top and bottom of the economizer. During the feature selection process, the use of both EIT1 and EIT2 as outputs, as well as using only one of the features was explored. It was discovered that the model with highest performance contained both EIT1 and EIT2.

Table 2 Model Input and Output Features

Inputs	**Outputs**
	P_{gen}
P_{req}	N
T_1	TOT
ΔP	COT
P_{amb}	COP
V_{wSat}	RIT_a
T_{wSatIn}	CCIT
T_{wIn}	EIT1
	EIT2

Generally, the ambient conditions of an MGT are important for its operation and efficiency. This means that the pressure and temperature before the compressor inlet can be of great importance in determining the values of other parameters. The test rig used for this study only measured T1 and ΔP, and so local weather data was obtained and used to give an idea of the ambient pressure in the area at the time of test runs.

Journal of Engineering for Gas Turbines and Power. Received July 18, 2023;
Accepted manuscript posted October 18, 2023. doi:10.1115/1.4063785

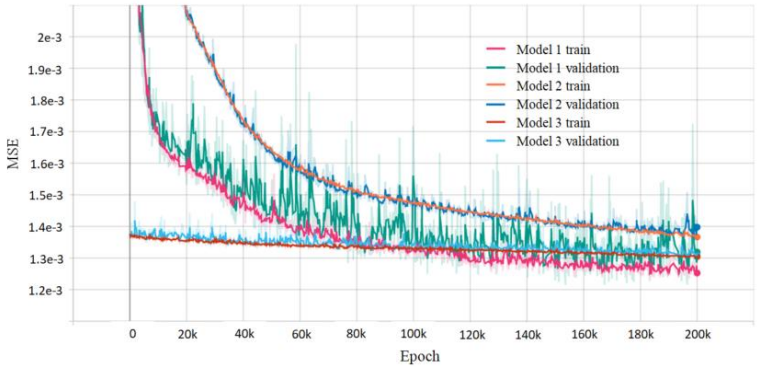

Figure 3 Model MSE Comparison varying learning rate

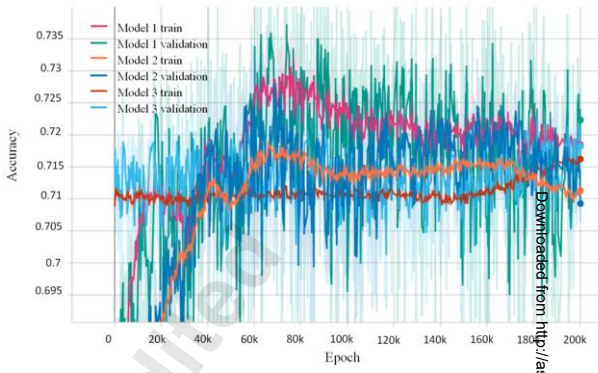

Figure 4 Model Accuracy Comparison

The frequency of data collection was 10Hz, which resulted in a significant amount of data. This is generally good for a data-driven method as the more data available the better the overall training process and ultimately a model which can generalize well. However, having such a high frequency can also lead to many outliers. Outliers are samples which lie out with a given range so differ significantly from other observations. This is undesirable, as it does not represent the true operation of the system, so data cleaning should be conducted to try and remove these points. On analyzing the data, it was found that ΔP and V_{wSat} had the most significant outliers and so these instances were removed from all input and output features to return a cleaner dataset.

As data had been obtained for both P_{amb} and ΔP, it was possible to combine these features to get a new combined input feature, which could resemble compressor inlet pressure (CIP). To ensure good features had been selected, the correlation between inputs and labels was explored. Python has a built-in function that allows the user to understand the linear correlations between parameters, which can help choose what parameters are relevant for the model. From this study, it was found that having CIP as an input had no better correlation to the outputs than using ΔP alone and so it was later removed.

Feature scaling is one of the most important steps in the data preparation process. As ML algorithms work best on numbers, they tend to assume that features with higher values have a greater influence on the outputs, which is not true in most cases. To avoid this, features should be scaled down. One of the most popular feature scaling methods is normalization, where all features are bound by the same range, usually [0,1] or [-1, 1], depending on the algorithm used. In this study, the tanh estimator and max-min normalization were explored. Tanh results in values between [-1,1], while max-min returns values in the range [0,1]. It was discovered that max-min normalization returned better results in the training process and so was utilized throughout.

Artificial Neural Network Training

After the data was properly processed the ANN could then be trained. A wide range of model parameters were altered to optimize performance, such as number of nodes in the hidden layer, learning rate, momentum, and activation function.

The number of nodes in the hidden layer was altered between 8 and 50 and it was discovered that using 35 nodes produced best results. Models with less than 8 nodes have been tested previously and were not able to fully capture the non-linear nature of the MGT operational parameters, and thus had much poorer performance. Considering that the GT performance strongly depends on weather conditions, special care must be taken when selecting the appropriate number of nodes. For some cases, a lower number of nodes may lead to better robustness and overall model performance. However, for this study it was discovered that a lower number of nodes was not suitable.

Additionally, the activation function of the hidden layer was altered between Sigmoid, Rectified Linear Unit (ReLU) and tanh. Tanh performed best and was used in the final model. It was decided to use mini-batch gradient descent (GD) as the optimizer and the loss algorithm used was MSE. Using mini-batch GD requires the training set to be split into smaller batches, where model parameters are updated after each batch is fed into the network. 1,000 samples were contained in each batch and so model parameters were updated 42 times in one epoch. Using batches can often decrease the overall training time, however it can also cause the loss function to oscillate more than if standard GD was used. During the model optimization process each model was trained for 100k epochs, before training the final model for 200k epochs.

Table 3 Final Model Settings

Input Nodes	7
Output Nodes	9
Hidden layers	1
Hidden nodes	35
Learning rate	0.1
Hidden Layer Activation Function	tanh
Optimizer	Mini-batch GD
Loss Algorithm	MSE
Metrics	Accuracy
Training size	40,111 samples
Batch Size	1,000 samples
Training epochs	200k

Figure 3 illustrates the difference in MSE between 3 different models. Each model had the same settings as that given in Table 3, however there was a change in the learning rate and training epochs. Model 1 was trained with a learning rate of 0.9 and 200k epochs. Given the high oscillations in MSE for model 1, a model with a lower learning

rate of 0.1, model 2, was trained to determine if this reduced the noise. Due to the decrease in loss oscillations, but increase in final MSE value, model 3 was then created by training model 2 for a further 200k epochs to understand if the MSE would continue to decrease.

Table 4 MSE and Accuracy Model Comparisons

Model	Training Loss	Training Accuracy	Validation Loss	Validation Accuracy
Model 1	1.2389e-3	0.7173	1.3585e-3	0.7274
Model 2	1.3658e-3	0.7112	1.4127e-3	0.7063
Model 3	1.304e-3	0.7165	1.3023e-3	0.7221

Table 6 Number (and percentage) of samples in each relative error bracket

Error (%)	Pgen	N	TOT	COT	COP	RITa	CCIT	EIT1	EIT2
<1	7909 (57.62%)	13599 (99.08%)	13725 (100%)	13550 (98.72%)	12463 (90.81%)	8063 (58.75%)	13658 (99.51%)	9747 (71.02%)	10128 (73.79%)
1-2	3956 (28.82%)	122 (0.89%)	0	173 (1.26%)	994 (7.24%)	3809 (27.75%)	67 (0.49%)	3041 (22.16%)	2765 (20.15%)
2-5	1817 (13.24%)	4 (0.03%)	0	2 (0.01%)	265 (1.93%)	1547 (11.27%)	0	874 (6.37%)	792 (5.77%)
5-10	43 (0.31%)	0	0	0	3 (0.02%)	234 (1.70%)	0	62 (0.45%)	39 (0.28%)
> 10	0	0	0	0	0	72 (0.52%)	0	1 (0.01%)	1 (0.01%)

The training and validation MSE and accuracy for each model is presented in Table 4. The model accuracy is calculated based on the number of times a model's prediction equals the label, where 1 implies that the model is 100% accurate on all predictions. Model 1 appears to have the lowest training loss and highest training accuracy. However, the validation loss is slightly higher than that of model 3 suggesting that it may overfit the training set slightly more. Also, Figure 3 and 4 portray that the MSE and accuracy for model 1 oscillates more than it does for the other models. This introduces some uncertainty in the accuracy of the model. Model 3 was trained for 200k more epochs than model 2, however the loss has started to plateau and there is not much improvement. It was then decided to use model 2 for the final model as it has low training and validation loss as well as high accuracy.

RESULTS AND DISCUSSION

Due to the reasons explained in the previous section, model 2 was used for making predictions on the test set. An evaluation of the model on the test set was conducted utilizing the same metrics as in the training and validation process. Comparing Table 4 and Table 5, the testing MSE lies between that of the training and validation, and so it can be confirmed that the model can generalize well. The accuracy is also slightly higher on the test set than that found during the training process.

Journal of Engineering for Gas Turbines and Power. Received July 18, 2023;
Accepted manuscript posted October 18, 2023. doi:10.1115/1.4063785

Table 5 Evaluation results of the test set

Testing MSE	**Testing Accuracy**	**MAE**
1.3744e-3	0.7159	0.0250

For the final predictions, the relative error (RE) was found, the results of which are presented in Table 6. The RE is the ratio of the absolute error to the expected measurement, given by Equation (1):

$$\delta = \left|\frac{predicted\ value - true\ value}{true\ value}\right| \times 100 \qquad (1)$$

This metric is more useful for evaluating the model on its capability to provide accurate predictions, than using MSE alone. From Table 6, the best performing features are N, COT, CCIT and TOT. All TOT predictions had a RE less than 1%, while CCIT and COT had only 1.27% and 0.49% of predictions greater than 1%, respectively. In total, less than 5% of the predictions have a RE greater than 2%. The differences between true and predicted values are visualized in Figures 5(a)-(h).

Journal of Engineering for Gas Turbines and Power. Received July 18, 2023;
Accepted manuscript posted October 18, 2023. doi:10.1115/1.4063785

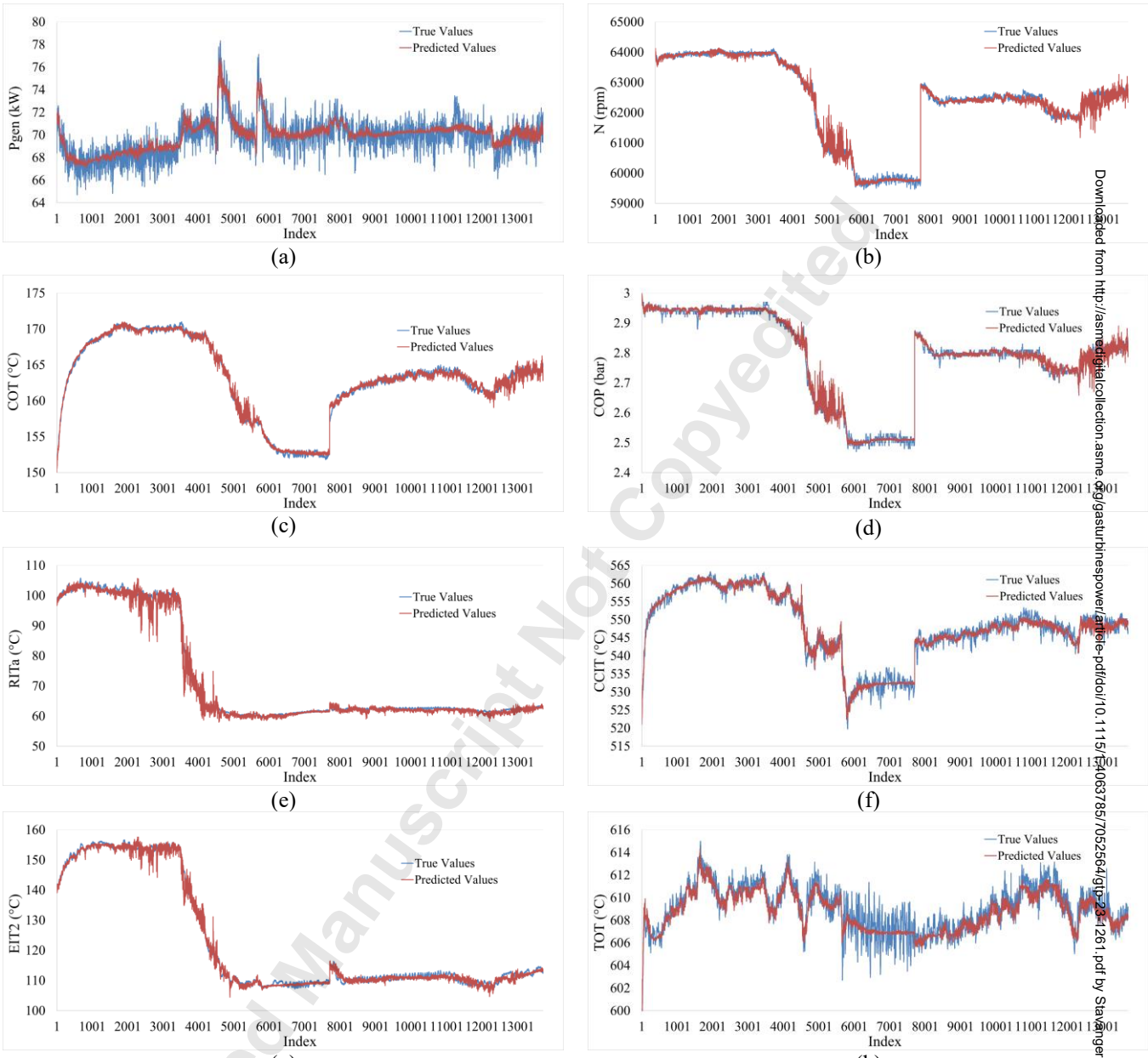

Figure 5 MLP model predicted outputs compared to true values

Certain features, for example RITa, did not have as high prediction accuracy. This could be due to the selected features not containing enough information to predict RITa well, or a possible problem in the collection of the data. From Figure 5(e), there is high oscillation in predicted values where the true labels appear to be smooth. This appears

to be where possible transient operation is. Further analysis should be done on the data and operation to improve prediction of transient operation.

Another poorly performing feature was P_{gen}, however on studying Figure 5(a), it is obvious that the true values of P_{gen} are very noisy and the MLP appears to smooth out these oscillations when making predictions. This suggests that with the features selected the algorithm can average out P_{gen}, even when data is noisy. It should be noted that the data obtained for P_{gen} is not measured data and is instead calculated, with a time delay, by the T100 system on the DC side of the power electronics. As the power electronics not only converts the electricity, it also controls the speed of the MGT, and so this action may intervene with the calculation. In future, to avoid the collection of highly oscillating data, real power sensors should be installed at the outlet of the power electronics to obtain more accurate power readings.

Given the success of this model on condition monitoring of an mHAT system, it is thought that the current model may work well for detecting compressor surge. It is suggested that the future model contains features which track the performance of the compressor such as T1 and Pamb as inputs, and COP and COT as outputs. As the addition of water into the system pushes the operating point closer to the surge margin, the amount of water in the system and the conditions of this water should be considered for surge prediction. Therefore, V_{wSat} and T_{wSatIn} would also be good feature choices. The poorer performance of RIT_a suggests that this feature may need to be disregarded in future, better inputs used, or better analysis of the operating conditions must be considered.

CONCLUSION

The objective of this study was to create a baseline ANN model for conducting condition monitoring in an mHAT system. In general, the model had high performance in predicting N, TOT, COT and CCIT, and also had acceptable results for COP, EIT1 and EIT2. From the results, it is clear to see that there may be some fast transient operation that the model did not manage to completely capture, which could be the reason for lower prediction accuracy for RIT_a. However, the obtained results illustrated that the ANN is able to predict the performance of the engine with very good accuracy and it is expected that further improvements in the prediction could be achieved. Future work should reassess the data and system operation allowing for a more accurate assessment into the performance of an MLP ANN on engine behavior. Another option would be to try another network, for example a recurrent neural network, which may be able to capture transient operation more clearly and thus have a higher performance and accuracy. Additionally, some of the data features were found to contain noise, which is likely to have influenced the overall

performance of the model, particularly for feature P_{gen}. It is hoped that in future, a method, such as a denoising autoencoder or signal processing, will be used to clean the data before feeding into the MLP to improve performance further.

The involved research groups believe that this model will provide a baseline for future studies involving condition monitoring and the detection of faults such as compressor surge.

REFERENCES

[1] I. Energy Agency, "Renewables 2021 - Analysis and forecast to 2026," 2021.

[2] U. Environmental Protection Agency, C. Heat, and P. Partnership, "Catalog of CHP Technologies, Section 5. Technology Characterization – Microturbines," 2015.

[3] H. Nikpey, M. Assadi, and P. Breuhaus, "Experimental Investigation of the Performance of a Micro Gas Turbine Fueled with Mixtures of Natural Gas and Biogas," 2013.

[4] H. Nikpey Somehsaraei, M. Mansouri Majoumerd, P. Breuhaus, and M. Assadi, "Performance analysis of a biogas-fueled micro gas turbine using a validated thermodynamic model," *Applied Thermal Engineering*, vol. 66, no. 1–2, pp. 181–190, 2014, doi: 10.1016/j.applthermaleng.2014.02.010.

[5] M. du Toit, N. Engelbrecht, S. P. Oelofse, and D. Bessarabov, "Performance evaluation and emissions reduction of a micro gas turbine via the co-combustion of H2/CH4/CO2 fuel blends," *Sustainable Energy Technologies and Assessments*, vol. 39, Jun. 2020, doi: 10.1016/j.seta.2020.100718.

[6] F. Reale, R. Calabria, F. Chiariello, R. Pagliara, and P. Massoli, "A Micro Gas Turbine Fuelled by Methane-Hydrogen Blends," *Applied Mechanics and Materials*, vol. 232, pp. 792–796, Nov. 2012.

[7] U.S. Department of Energy, Office of Energy Efficiency and Renewable Energy, and Office of Power Technologies., "Advanced Microturbine Systems - Program plan for fiscal years 2000 through 2006. 2000."

[8] W. de Paepe, M. M. Carrero, S. Bram, A. Parente, and F. Contino, "Toward higher micro gas turbine efficiency and flexibility-humidified micro gas turbines: A review," *Journal of Engineering for Gas Turbines and Power*, vol. 140, no. 8, Aug. 2018, doi: 10.1115/1.4038365.

[9] H. Nikpey, M. M. Majoumerd, M. Assadi, and P. Breuhaus, "Thermodynamic Analysis of Innovative Micro Gas Turbine Cycles," 2014.

[10] H. Nikpey Somehsaraei *et al.*, "Evaluation of a Micro Gas Turbine with Post-combustion CO2 Capture for Exhaust Gas Recirculation Potential with Two Experimentally Validated Models," 2017.

[11] W. de Paepe, M. M. Carrero, S. Bram, and F. Contino, "T100 Micro Gas Turbine Converted to Full Humid Air Operation: A Thermodynamic Performance Analysis," 2015.

[12] M. Montero Carrero, W. de Paepe, J. Magnusson, A. Parente, S. Bram, and F. Contino, "Experimental characterisation of a micro Humid Air Turbine: assessment of the thermodynamic performance," *Applied Thermal Engineering*, vol. 118, pp. 796–806, 2017, doi: 10.1016/j.applthermaleng.2017.03.017.

[13] W. de Paepe, S. Giorgetti, M. Montero Carrero, S. Bram, A. Parente, and F. Contino, "Towards Highly-Flexible Carbon-Clean Power Production using Gas Turbines: Exhaust Recirculation and cycle Humidification," 2018.

[14] W. de Paepe, F. Delattin, S. Bram, E. Brussel, F. Contino, and J. de Ruyck, "A Study on the Performance of Steam Injection in a Typical Micro Gas Turbine," 2013. [Online]. Available: http://asmedigitalcollection.asme.org/GT/proceedings-pdf/GT2013/55195/V05AT23A011/4223446/v05at23a011-gt2013-94569.pdf

[15] A. Belokon, K. Khritov, L. Klyachko, S. Tschepin, V. Zakharov, and G. Jr. Opdyke, "Prediction of Combustion Efficiency and NOx Levels for Diffusion Flame Combustors in HAT Cycles," in *ASME Turbo Expo*, Jun. 2002, pp. 791–797.

[16] M. Ferrarotti, W. de Paepe, and A. Parente, "Reactive structures and NOx emissions of methane/hydrogen mixtures in flameless combustion," *International Journal of Hydrogen Energy*, vol. 46, no. 68, pp. 34018–34045, Oct. 2021, doi: 10.1016/j.ijhydene.2021.07.161.

[17] W. de Paepe, P. Sayad, S. Bram, J. Klingmann, and F. Contino, "Experimental Investigation of the Effect of Steam Dilution on the Combustion of Methane for Humidified Micro Gas Turbine Applications," *Combustion Science and Technology*, vol. 188, no. 8, pp. 1199–1219, Aug. 2016, doi: 10.1080/00102202.2016.1174116.

[18] S. G. ¨ Oke *et al.*, "Influence of Pressure and Steam Dilution on NOx and CO Emissions in a Premixed Natural Gas Flame," 2013. [Online]. Available: http://asmedigitalcollection.asme.org/GT/proceedings-pdf/GT2013/55102/V01AT04A056/4222249/v01at04a056-gt2013-94782.pdf

[19] M. Montero Carrero, M. Luigi Ferrari, W. de Paepe, and A. Parente, "Transient Simulations of a T100 Micro Gas Turbine Converted into a Micro Humid Air Turbine," 2015. [Online]. Available:

http://asmedigitalcollection.asme.org/GT/proceedings-pdf/GT2015/56673/V003T06A016/4236169/v003t06a016-gt2015-43277.pdf

[20] W. de Paepe, M. M. Carrero, S. Bram, and F. Contino, "T100 Micro Gas Turbine Converted to Full Humid Air Operation: Test Rig Evaluation."

[21] H. HANACHI, J. LIU, and C. MECHEFSKE, "Multi-mode diagnosis of a gas turbine engine using an adaptive neuro-fuzzy system," *Chinese Journal of Aeronautics*, vol. 31, no. 1, pp. 1–9, Jan. 2018, doi: 10.1016/j.cja.2017.11.017.

[22] H. Nikpey, M. Assadi, and P. Breuhaus, "Development of an optimized artificial neural network model for combined heat and power micro gas turbines," *Applied Energy*, vol. 108, pp. 137–148, 2013, doi: 10.1016/j.apenergy.2013.03.016.

[23] G. R. Matuck, J. R. Barbosa, C. Bringhenti, and I. Lima, "Multiple Faults Detection of Gas Turbine by MLP Neural Network."

[24] T. Palmé, M. Fast, and M. Thern, "Gas turbine sensor validation through classification with artificial neural networks," *Applied Energy*, vol. 88, no. 11, pp. 3898–3904, 2011, doi: 10.1016/j.apenergy.2011.03.047.

[25] J. E. Yoon, J. J. Lee, T. S. Kim, and J. L. Sohn, "Analysis of performance deterioration of a micro gas turbine and the use of neural network for predicting deteriorated component characteristics," *Journal of Mechanical Science and Technology*, vol. 22, no. 12, pp. 2516–2525, Dec. 2008, doi: 10.1007/s12206-008-0808-8.

[26] M. R. Hamouda, M. I. Marei, M. E. Nassar, and M. M. A. Salama, "ANN-supervised Interface System for Microturbine Distributed Generator," in *Canadian Conference on Electrical and Computer Engineering*, Aug. 2020, vol. 2020-August. doi: 10.1109/CCECE47787.2020.9255730.

[27] W. de Paepe, F. Contino, F. Delattin, S. Bram, and J. de Ruyck, "New concept of spray saturation tower for micro Humid Air Turbine applications," *Applied Energy*, vol. 130, pp. 723–737, Oct. 2014, doi: 10.1016/j.apenergy.2014.03.055.

[28] W. de Paepe, A. Pappa, D. Coppitters, M. M. Carrero, P. Tsirikoglou, and F. Contino, "Recuperator performance assessment in humidified micro gas turbine applications using experimental data extended with preliminary support vector regression model analysis," *Journal of Engineering for Gas Turbines and Power*, vol. 143, no. 7, Jul. 2021, doi: 10.1115/1.4049266.

[29] W. de Paepe, A. Pappa, D. Coppitters, M. M. Carrero, P. Tsirikoglou, and F. Contino, "Control Strategy Development for Optimized Operational Flexibility from Humidified Micro Gas Turbine: Saturation Tower Performance Assessment."

[30] W. de Paepe, M. M. Carrero, S. Bram, and F. Contino, "T100 MICRO GAS TURBINE CONVERTED TO FULL HUMID AIR OPERATION: TEST RIG EVALUATION." [Online]. Available: http://asmedigitalcollection.asme.org/GT/proceedings-pdf/GT2014/45653/V03AT07A020/4230988/v03at07a020-gt2014-26123.pdf

[31] W. de Paepe, "Flexible Heat Production from a micro Gas Turbine," 2014.